Bremer, K., Reinsch, T., Leen, G., Roth, B., Lochmann, S., Lewis, E. (2017): Pressure, temperature and refractive index determination of fluids using a single fibre optic point sensor. - *Sensors and Actuators A - Physical*, *256*, pp. 84—88.

DOI: http://doi.org/10.1016/j.sna.2017.01.025

Pressure, temperature and refractive index determination of fluids using a single fibre optic point sensor

K. Bremer[1*], T. Reinsch[2], G. Leen[4], B. Roth[1], S. Lochmann[3], E. Lewis[4]

[1] Hannover Center for Optical Technologies (HOT), Leibniz Universitaet Hannover, Hanover, Germany

[2] GFZ German Research Centre for Geosciences GFZ, Potsdam, Germany

[3] Communications Signal Processing Group, Hochschule Wismar, Wismar, Germany

[4] Optical Fibre Sensor Research Centre (OFSRC), University of Limerick, Limerick, Ireland

Corresponding author: Kort Bremer
Hannover Centre of Optical Technologies
Leibniz University Hannover
Nienburger Straße 17
D-30167 Hannover, Germany
Kort.Bremer@hot.uni-hannover.de
Phone: +49 511 762 17905

Abstract: The accurate determination of physico-chemical fluid parameters is of major importance in many process engineering applications. Not only the monitoring of the phase distribution in piping systems but also the detection of chemical concentrations in liquids is of interest for an efficient, safe and reliable operation of laboratory as well as industry scale applications. In this paper, we present a miniature all-silica fiber optic sensor capable of measuring pressure, temperature and refractive index of a fluid at a single point simultaneously. In future, such a sensor can be utilized in applications, where these quantities and, hence, phase composition or chemical concentration have to be monitored possibly under harsh environments such as geothermal or oil drilling wells.

1. Introduction

Pressure, temperature and refractive index of a medium are not independent variables [1][2]. For a salt solution, e.g. seawater, the refractive index (RI) n is a function of pressure p, temperature T, concentration c, as well as the wavelength of the incident light λ, n(p,T,c, λ) [3][4][5]. Determining pressure, temperature, and refractive index of a solution of known salt composition by using laser radiation with known wavelength, the salt concentration can be determined. Another relevant monitoring application is the determination of the phase composition of a fluid within a geothermal well or oil well. Since the refractive index of a substance in the liquid phase is significantly different from that in the gas phase such a sensor can be used to monitor the exact phase composition of a fluid. Whether a single phase or a two phase fluid is produced from different geological horizons, for example, it will have a significant influence on the exploitation strategy for such a well.

In many laboratory as well as industry scale applications monitoring of chemical processes, especially dissolution and precipitation reactions or reactions involving a changing phase, it is of major importance to investigate, understand, and control, the relevant processes. Monitoring of such processes is especially important in high temperature (e.g. > 150 °C) and in high pressure conditions (e.g. > 10 MPa), for example, in geothermal applications [6]. However, many conventional sensor systems have difficulties operating under such conditions due to the operational temperature limit of available electronic components.

A potential solution is the use of fibre optic sensors, which have the inherent advantages of being tolerant of high temperatures and pressures, miniature in size, resistant to corrosion, electrically passive, multiplexable as well as capable of being operated remotely. In the past, several different fibre optic sensors have been designed to simultaneously measure pressure and RI or temperature and RI. For instance, to determine temperature and RI simultaneously several different systems such as a partially cone-shaped Fibre Bragg Grating (FBG) [7], an in-line Mach-Zehnder Interferometer (MZI) embedded in a FBG [8], a core-offset MZI combined with a FBG [9] or a Long Period Grating (LPG) based MZI [10] have been reported. Also a fibre optic sensor based on a SU-8 sensor tip [11], a dual-cavity Fabry-Perot Interferometer (FPI)[12][13] or a temperature-insensitive FPI relying on a photonic-crystal fibre [14] have been proposed. To measure both pressure and RI a combination of an open path and pressure sensitive cavity FPI has been described [15]. However, to date only one fibre optic sensor concept has been reported to simultaneously measure pressure, temperature and RI [16]. The fibre optic sensor consists of a sophisticated multi-cavity sapphire transducer, where a diaphragm cavity, a pressure sensing cavity and a base cavity are used to determine all three parameters.

In previous work we demonstrated the simultaneous measurement of pressure and temperature for pressures up to 30 MPa [17] and temperatures up to 430 °C [18] by using a fibre optic Extrinsic Fabry-Perot Interferometer (EFPI) sensor which contains an embedded Fibre Bragg Grating (FBG) reference sensor element. The sensor design has also been successfully tested up to 70 MPa under isothermal conditions [19]. In this work we investigate, for the first time, the additional measurement of the RI of the surrounding medium. Based on the the all-silica structure and the capability to simultaneously measure pressure, temperature and RI, the multi-parameter fibre optic sensor can, in the future, be deployed in harsh environmental conditions, as the ones experienced in chemical process monitoring or downhole geothermal applications.

2. Theoretical Background

2.1 Principle of Operation

A schematic of the multi-parameter fibre optic sensor is illustrated in Fig. 1, see e.g. [17] for details. The sensor head is entirely fabricated from fused-silica elements, i.e. it is completely made from glass. The sensor is realized by splicing a 200 µm silica glass fibre and a Single-Mode (SM) fibre which has an embedded FBG to both sides of a 133 µm/220 µm (inner/outer diameter) silica glass capillary. The splicing is achieved by using a conventional fusion splicer (BIT MM-40). The EFPI element is fabricated at the sensor head by cleaving and polishing the 200 µm fibre such that it is several tens or hundreds of micrometers from the glass capillary/200 µm fibre splice.

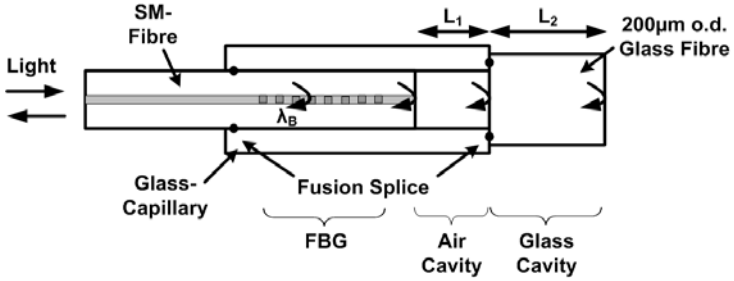

Fig. 1: Schematic multi parameter fibre optic sensor

The operation of the multi-sensor is as follows: light of intensity I_0, propagates to the sensor head via the SM-Fibre, a wavelength component of this light is reflected at the FBG, the reflected wavelength being equal to the Bragg wavelength λ_B. All other wavelength components propagate through the FBG and are reflected at three locations: a) the glass/air interface of the SM fibre (A_{01}); b) the air/glass interface of the 200 µm fibre (A_{12}) and c)the interface between the 200 µm fibre and the surrounding medium (A_{23}). All three reflections propagate back into the SM fibre and return to the interrogation instrumentation. Due to the low reflection coefficients of A_{01}, A_{12} and A_{23} and neglecting any interference between the FBG and the reflections of the EFPI cavities, the reflected sensor spectrum can be calculated as [20]:

$$\frac{I(\lambda)}{I_0} = R_{FBG}(\lambda - \lambda_B) \cdot \left[\begin{array}{l} A_{01}^2 + A_{12}^2 + A_{23}^2 - 2A_{01}A_{12}\cos\left(\frac{4\pi L_1}{\lambda}\right) \\ + 2A_{01}A_{23}\cos\left(\frac{4\pi(L_1 + n_2 L_2)}{\lambda}\right) - 2A_{12}A_{23}\cos\left(\frac{4\pi n_2 L_2}{\lambda}\right) \end{array} \right] \quad (1)$$

where n_2 is the refractive index of the 200 µm optical fibre, λ is the free space optical wavelength and L_1 and L_2 are the length of the EFPI air cavity and glass cavity, respectively. The amplitudes A_{01}, A_{12} and A_{23} of the reflected light within the EFPI cavity can be calculated as $A_{01} = r_{01}$, $A_{12} = \eta_1 \cdot T_{01} \cdot r_{12}$ and $A_{23} = \eta_2 \cdot T_{01} \cdot T_{12} \cdot r_{23}$, where η_1, η_2, T_{01} and T_{12} are the coupling coefficient of the cavities and the power transmission coefficient of the glass/air interfaces. The reflectivities of the glass/air interface r_{01} and air/glass interface r_{12} can be specified as 0.184 and -0.182 for $n_0 = 1.4504$ [21] and $n_2 = 1.445$. The reflectivity r_{23} of the outer end-face of the 200 µm optical fibre depends on the refractive index of the surrounding medium and can be calculated using the Fresnel law as:

$$r_{23} = (n_2 - n_{med})/(n_2 + n_{med}), \quad (2)$$

where n_{med} is the refractive index of the surrounding medium.

2.2 Gaussian beam divergence within the sensor cavities

As the fundamental mode of the SM-fibre can be approximated by a Gaussian distribution of a transverse and linear polarised electric field, the coupling coefficients of the cavities η_1 and η_2 can be determined by applying Gaussian beam divergence. The coupling coefficients are defined as [22]:

$$\eta_x^2 = \left(\frac{2 \cdot \omega_0 \cdot \omega_x}{\omega_0^2 + \omega_x^2} \right)^2 \text{ , with x = 1 or 2.} \quad (3)$$

In Equations 3, ω_0 is the spot size of the Gaussian beam at the end-face of the SM fibre and can be calculated as: $\omega_0 = a \cdot (0.65 + 1.619 \cdot V^{-3/2} + 2.879 \cdot V^{-6})$ [22]; where a and V are the core radius and normalised frequency of the SM fibre and defined as a = 4.1µm and V = 2.16 for the Corning fibre SMF28 [21]. Furthermore, ω_1 specifies the spot size of the Gaussian beam radius after crossing the EFPI air cavity only, whereas ω_2 is the spot size of the Gaussian beam radius after crossing the air and glass cavity of the multi-parameter fiber optic sensor. Both spot sizes ω_1 and ω_2 can be calculated as [23][24]:

$$\omega_1(z) = \omega_0 \sqrt{1 + \left(\frac{2L_1 \cdot \lambda}{\pi \cdot \omega_0^2} \right)^2} \quad (4a)$$

$$\omega_2(z) = \omega_0 \sqrt{1 + \left(\frac{(2L_1 + 2L_2 / n_2) \cdot \lambda}{\pi \cdot \omega_0^2} \right)^2} \tag{4b}$$

As soon as the Gaussian beam propagates through the cavities, its diameter increases while the power density, and hence the coupling coefficients, decrease, and can be associated with losses within the cavity. Furthermore, both coupling coefficients depend on the length of the cavities.

3. Additional refractive index sensing

3.1 Refractive index determination of the surrounding medium

The refractive index of the surrounding medium can be obtained by determining the reflection r_{23} at the end-face of the 200 µm fibre, as given in Equation 2. In the case of the multi-parameter fibre optic sensor, the reflection r_{23} was obtained by calculating the ratio γ between the amplitude of the second cosine term and the amplitude of the first cosine term in Equation 1, as opposed to determining r_{23} and hence the RI of the surrounding directly from the amplitude of second or third cosine term of Equation 1. This calculation makes the obtained RI measurement independent of light source fluctuation and attenuation variation along the fibre optic link. Therefore, r_{23} can be determined as:

$$\gamma = \frac{2A_{01}A_{23}}{2A_{01}A_{12}} = \frac{\eta_2 \cdot T_{12}}{\eta_1 \cdot r_{12}} \cdot r_{23} \tag{5}$$

3.2 Cross-sensitivity to applied pressure and temperature

From Equation 5 it follows that the measurement range and sensitivity of γ depends strongly on the coupling coefficients η_1 as well as η_2 and thus on the length of the cavities L_1 and L_2. In Fig. 2 the sensitivity of γ to η_1 and η_2 is visualised for r_{23} = 0.182 (n_{med} = 1). As illustrated in Fig. 2, maximum values for γ are achieved for small L_2, because in this case η_1 and η_2 are almost identical and hence they cancel each other out. However, since the sensor is designed to measure high pressure values the thickness (length) L_2 of the 200 µm silica glass fibre needs to be selected appropriately to withstand high pressure environments.

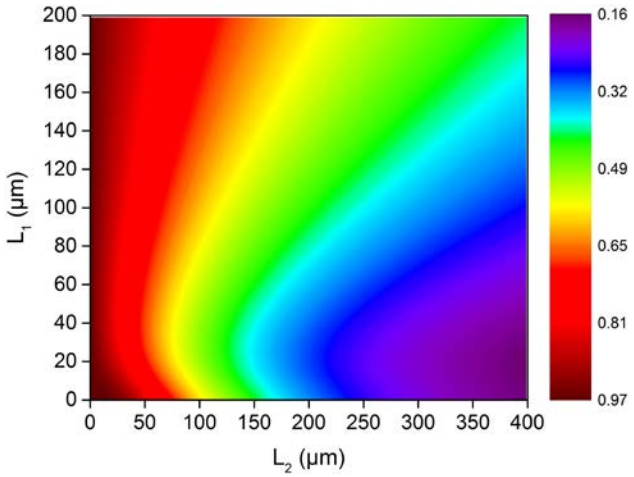

Fig. 2: Simulation of γ as a function of the EFPI air and glass cavity lengths L_1 and L_2.

Moreover, as γ is sensitive to the EFPI cavity lengths L_1 and L_2, applied pressure, as well as temperature, cavity length changes introduce an error when measuring the RI of the surrounding medium. As investigated in [17] the change of the EFPI air cavity length depends linearly on a change of applied pressure $\Delta L_1 \sim \Delta P$ (0.054µm/MPa) and temperature $\Delta L_1 \sim \Delta T$ ($1.9 \cdot 10^{-4}$ µm/°C). Moreover, the length change of the EFPI glass cavity due to applied pressure and temperature can be calculated as $9.1 \cdot 10^{-6}$ L_2/MPa and $5 \cdot 10^{-7}$ L_2/°C for silica glass [25], respectively. Therefore, the introduced error ϵ of the fringe visibility measurement due to applied pressure and applied temperature can be estimated using the following error analysis:

$$\varepsilon_P = \frac{\Delta\gamma}{FS \cdot MPa} \cdot 100\% = \left(\left| \frac{d\gamma}{dL_1} \right| \cdot 0.054 \mu m / MPa + \left| \frac{d\gamma}{dL_2} \right| \cdot 9.1 \cdot 10^{-6} \cdot L_2 / MPa \right) \cdot \frac{100\%}{FS} \quad (5a)$$

$$\varepsilon_T = \frac{\Delta\gamma}{FS \cdot °C} \cdot 100\% = \left(\left| \frac{d\gamma}{dL_1} \right| \cdot 1.9 \cdot 10^{-4} \mu m / °C + \left| \frac{d\gamma}{dL_2} \right| \cdot 5 \cdot 10^{-7} \cdot L_2 / °C \right) \cdot \frac{100\%}{FS} \quad (5b)$$

In Equation 5 the induced error is normalised to the Full-Scale (FS) of γ, where FS is defined for a RI measurement between n_{med} = 1 and n_{med} = n_{Silica}. In Fig. 3a and 3b the results of the simulation of Equation 5a and 5b are visualised.

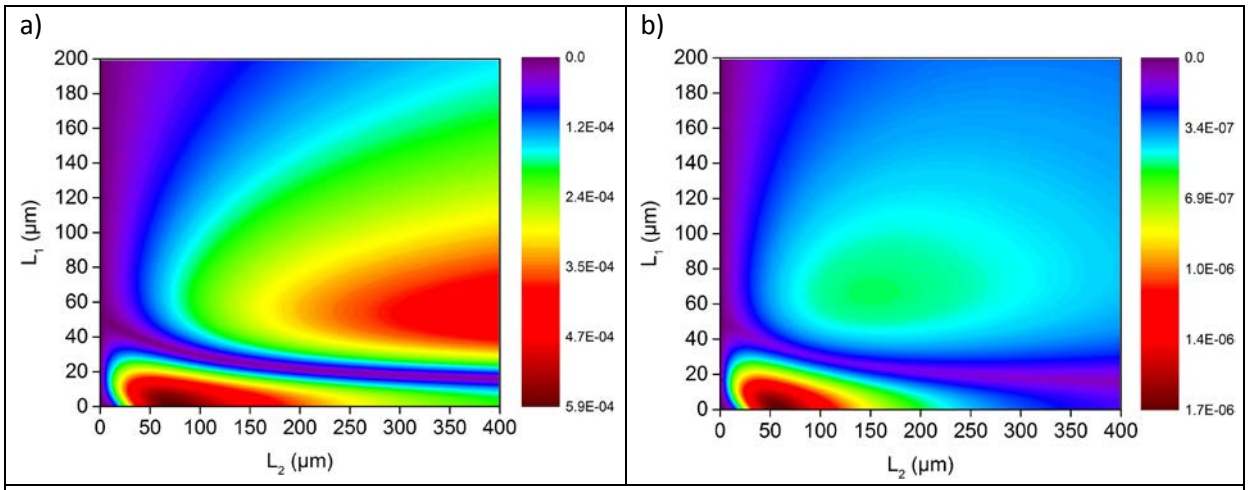

Fig. 3: Simulated cross-sensitivity of γ to (a) applied pressure (unit: %/MPa) and (b) applied temperature (unit %/°C)

From the simulation in Fig. 3 it follows that the length of the EFPI air and glass cavities can be optimised in order to eliminate the cross-sensitivity of the RI measurement to applied pressure and applied temperature. As a general rule of thumb, the air cavity length L_1 and the glass cavity length L_2 should be > 20 µm and < 250 µm, respectively, in order to minimize the cross-sensitivity to applied pressure and temperature as well as to optimize the sensitivity of γ.

4. Evaluation sensitivity to refractive index

For the evaluation of the sensor performance to applied refractive index, a multi-parameter fibre optic sensor was fabricated with a Bragg-wavelength of 1558.54 nm as well as an EFPI air and glass cavity of L_1 = 65 µm and L_2 = 220 µm. The selected cavity lengths L_1 and L_2 represent a trade-off in terms of the performance of determining the RI of the surrounding on one side and the sensor interrogation using the interrogation set-up and signal processing algorithm applied on the other side. The multi-parameter fibre optic sensor was interrogated using the interrogation system as reported previously [17], which consist on a broadband light Source (BBS) (INO FBS-C), an optical

circulator as well as an optical spectrum analyser (Ando AQ6330). Moreover, as described in Section 3, γ and hence the RI of the surrounding were determined by calculating the ratio between the amplitudes of the second and first cosine term of Equation 1. Both amplitudes were determined by calculating the Fast Fourier-Transform (FFT) of the measured reflected sensor spectrum. The resolution of the FFT was optimised by applying a Kaiser-window and Zero-Padding.

In order to obtain different RI values, five different solutions with different sodium chloride (NaCl) concentrations were prepared at different temperatures. The different concentrations of NaCl together with the corresponding refractive indices at the different temperatures are given in Table 1. The refractive indices were measured using the FRI Refractive Index Sensor from FISO Technologies Inc.

Concentration (mol/l)	**n(20°C)**	**n(40°C)**	**n(60°C)**	**n(80°C)**
0	1.3295	1.3272	1.3242	1.3207
1	1.3393	1.3366	1.3334	1.3300
2	1.3484	1.3457	1.3426	1.3392
3	1.3567	1.3538	1.3506	1.3476
4	1.3648	1.3618	1.3588	1.3557

Table 1 Concentration of NaCl solutions and corresponding refractive indices.

The performance of the multiple-parameter sensor to RI measurement was evaluated by inserting the sensor sequentially into the different NaCl solutions for each temperature value. Between every measurement the sensor was carefully rinsed using distilled water.

In Fig. 4 the obtained fringe visibility at different refractive index (at different NaCl concentrations and different temperatures) is shown. A linear response of the fringe visibility to RI changes between 1.32 and 1.365 was obtained. Furthermore, the cross-sensitivity of the calculated fringe visibility to temperature variations in the range from 20°C to 80°C can be neglected, which is consistent with the simulation from Fig. 3b. According to Fig. 4, a sensitivity of 0.58/RIU with a standard deviation at atmospheric pressure of $1.77 \cdot 10^{-3}$ RIU for temperatures ranging from 20°C to 80°C is obtained. From the simulation, a sensitivity of 0.69/RIU was calculated. The deviation between calculated and measured sensitivity can be explained by small misalignment of the fibre surfaces relative to each other and hence a decrease of the actual fringe visibility. For a confidence interval of 95% a sensor resolution of $\pm 5.98 \cdot 10^{-3}$ RIU is calculated. The sensor resolution can be further enhanced by optimizing the fringe visibility of the sensor, as illustrated in Fig. 2, as well as the sensor interrogation system.

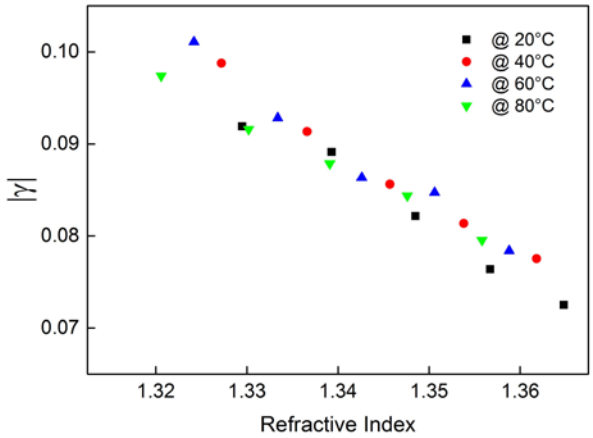

Fig. 4: Measured fringe visibility as a function of the corresponding RI.

5. Summary

In this work, an all-silica miniature fibre optic pressure and temperature sensor was extended to additionally measure refractive index of the surrounding medium. Experiments verified that the fringe visibility of the EFPI glass cavity is sensitive to the RI of the surrounding medium. The sensor tested shows a linear response of 0.58/RIU for the fringe visibility in the RI range from 1.32 to 1.365 with a standard deviation at atmospheric pressure of $1.77 \cdot 10^{-3}$ and in the temperature range from 20 °C to 80°C. Moreover, simulations in Section 3 were carried out to demonstrate that by choosing appropriate EFPI air and glass cavity length the cross-sensitivity of the RI measurement to applied pressure and temperature variations can be eliminated. Consequently, the sensor can be applied to measure pressure, temperature and RI simultaneously. The determination all three parameters will be investigated in lab-environment in the future.

Consequently, due to the all-silica structure and the capability to simultaneously measure pressure, temperature and RI, the multi-parameter fibre optic sensor reported in this work has the potential to be deployed in harsh environmental conditions, as, for example, the ones in chemical process monitoring or downhole geothermal applications. However, for a long term application in hostile environments like downhole applications suitable strategies for the lead optical fiber as well as the sensor packaging have to be developed [26][27].

The design of the presented sensor can be regarded as modular. In the current configuration, the sensitivity to refractive index was investigated. However, special coatings can be applied in the next version of the sensor system which are sensitive to changing environmental conditions, such as variation of pH levels or concentration of a specific ion species. The sensor can be tailored for different monitoring applications, where temperature, pressure and a chemical parameters need to be measured simultaneously.

Acknowledgment

The development of the multi sensor was supported in part by the Science Foundation Ireland grant SFI/ENEF662 and the IRCSET Embark Initiative. This work was also performed within the GeoEn Phase II project and funded by the German Federal Ministry of Education and Research (Grant Number 03G0767A) as well as the Gebo project ZN2481 funded by the Niedersächsisches Ministerium für Wissenschaft und Kultur (MWK). The authors would like to thank Cornelia Schmidt-Hattenberger, Mikaela Weiner, Christian Cunow and Tanja Ballerstedt from the German Research Centre for Geosciences for their support during the refractive index measurements.

Literature

[1] I. Thormahlen, J. Straub, U. Grigull, „Refractive Index of Water and Its Dependence on Wavelength, Temperature, and Density“, Journal of Physical and Chemical Reference Data 14 (1985) 933-945

[2] P. Schiebener, J. Straub, J. M. H. Levelt Sengers, J. S. Gallagher, „Refractive index of water and steam as function of wavelength, temperature and density“, Journal of Physical and Chemical Reference Data 19 (1990) 677-717

[3] J. V. Leyendekkers, “Prediction of the refractive index of seawater as a function of temperature, pressure, salinity and wavelength,” Marine Chemistry 5 (1977) 29–42

[4] G. A. Seaver, “The index of refraction to specific volume relation for sea water-a linearized equation of state,” Journal of Physical Oceanography 15 (1985) 1339–1343 (1985)

[5] R. C. Millard, G. Seaver, “An index of refraction algorithm for seawater over temperature, pressure, salinity, density, andwavelength,” Deep-Sea Research Part A-Oceanographic Research Papers 37 (1990) 1909–1926

[6] G. Blöcher, T. Reinsch, J. Henninges, H. Milsch, S. Regenspurg, J. Kummerow, H. Francke, S. Kranz, A. Saadat, G. Zimmermann, E. Huenges, "Hydraulic history and current state of the deep geothermal reservoir Groß Schönebeck Geothermics", accepted for publication

[7] C.-L- Zhao, L. Qi, S. Zhang, Y. Jin, S. Jin, „Simultaneous measurement of refractive index and temperature based on a partial cone-shaped FBG“, Sensors & Actuators B 178 (2013) 96 – 100

[8] C. R. Liao, Y. Wang, D. N. Wang, M. W. Yang, „Fiber in-line Mach-Zehnder interferometer embedded in FBG for simultaneous refractive index and temperature measurement“, IEEE Photonics Technology Letters 22 (2010) 1686-1688

[9] Q. Yao, H. Meng, W. Wang, H. Xue, R. Xiong, B. Huang, C. Tan, X. Huang, „Simultaneous measurement of refractive index and temperature based on a core-offset Mach-Zehnder interferometer combined with a fiber Bragg grating“, Sensors & Actuators A 209 (2014) 73-77

[10] M. Xiong, H. Gong, Z. Wang, C. Zhao, X. Dong, "Simultaneous Refractive Index and Temperature Measurement Based on Mach–Zehnder Interferometer Concatenating Two Bi-Tapers and a Long-Period Grating", IEEE Sensors Journal 16 (2016) 4295 - 4299

[11] M. Li, Y. Liu, S. Qu, Y. Li, “Fiber-optic sensor tip for measuring temperature and liquid refractive index”, Optical Engineering 53 (2014) 116110

[12] S. Pevec, D. Donlagic, “High resolution, all-fiber, micro-machined sensor for simultaneous measurement of refractive index and temperature”, Optics Express 22 (2014) 16241-16253

[13] H. Y. Choi, G. Mudhana, K. S. Park, U. Paek, B. H. Lee, “Corss-talk free and ultra-compact fiber optic sensor for simultaneous measurement of temperature and refractive index”, Optics Express 18 (2009) 141-149

[14] Y. Wang, D. N. Wang, C. R. Liao, T. Hu, J. Guo, H. Wei, „Temperature-insensitive refractive index sensing by use of micro Fabry-Perot cavity based on ximplified hollow-core photonic crystal fiber“, Optics Letters 38 (2013) 269-271

[15] S. Pevec, D. Donlagic, “Miniature fiber-optic sensor for simultaneous measurement of pressure and refractive index”, Optics Letters 39 (2014) 6221-6224

[16] R. D. Pechstedt, “Fibre optical sensor for simultaneous measurement of pressure, temperature and refractive index”, Proc. SPIE 91570I (2014) 1-4

[17] K. Bremer, B. Moss, G. Leen, E. Lewis, S. Lochmann, I. Mueller, T. Reinsch, J. Schroetter, „Fibre Optic Pressure and Temperature Sensor for Geothermal Wells“, IEEE Sensors 2010 Conference (2010) 538-541

[18]K. Bremer, E. Lewis, G. Leen, B. Moss, S. Lochmann, I. Mueller, “Feedback Stabilized Interrogation Technique for EFPI/FBG Hybrid Fiber-Optic Pressure and Temperature Sensors” IEEE Sensors Journal 12 (2012) 133-138

[19]T. Reinsch, G. Bloecher, H. Milsch, K. Bremer, E. Lewis, G. Leen, S. Lochmann, “A fibre optic sensor for the in situ determination of rock physical properties”, International Journal of Rock Mechanics and Mining Sciences 55 (2012) 55-62

[20]Y. Zhu, A. Wang, “Miniature Fiber-Optic Pressure Sensor”, IEEE Photonic Technology Letters 17 (2005) 447-449

[21]R. Wang, G. Farrell, Q. Wang, G. Rajan, „An optimized macrobending fiber based edge filter“, Photonics Technology Letters 19 (2007) 1136-1138

[22]D. Marcuse, “Loss Analysis of single-mode fiber splices”, The Bell System Technical Journal 56 (1997) 703-718

[23]A. Yariv, “Optical Electronics”, fourth ed., Saunders College Publishing, Philadelphia, 1991

[24]A. Yariv, “Solutions manual for optical electronics in modern communications”, fifth ed., Oxford Univ. Press, New York, 1997

[25]G. B. Hocker, “Fiber-optic sensing of pressure and temperature”, Applied Optics 18 (1979) 1445-1448

[26]T. Reinsch, J. Henninges, R. Ásmundsson, " Thermal, mechanical and chemical influences on the performance of optical fibres for distributed temperature sensing in a hot geothermal well", Environmental Earth Sciences 70 (2013) 3465-3480

[27]T. Reinsch, J. Henninges, " Temperature-dependent characterization of optical fibres for distributed temperature sensing in hot geothermal wells", Measurement Science and Technology 21 (2010) 094022